2020년 8월

석사학위 논문

Inhibition of RANKL-induced osteoclastogenesis by novel mutant RANKL

조 선 대 학 교 대 학 원

의 과 학 과

장 유 리 아

Inhibition of RANKL-induced osteoclastogenesis by novel mutant RANKL

신규mutant RANKL에 의한 파골세포 활성 억제 효과

2020년 8월 28일

조 선 대 학 교 대 학 원

의 과 학 과

장 유 리 아

Inhibition of RANKL-induced osteoclastogenesis by novel mutant RANKL

지도교수 임 원 봉

이 논문을 약학 석사학위신청 논문으로 제출함

2020년 5월

조 선 대 학 교 대 학 원

의 과 학 과

장 유 리 아

장유리아의 석사학위 논문을 인준함

위원장 조선대학교 교수 손 홍 문 (인)

위 원 조선대학교 교수 김 동 휘 (인)

위 원 조선대학교 교수 임 원 봉 (인)

2020년 6월

조 선 대 학 교 대 학 원

CONTENTS

LIST OF FIGURES

ABSTRACT

신규mutant RANKL에 의한 파골세포 활성 억제 효과

장 유 리 아

지도교수 : 임 원 봉

조선대학교 대학원 의과학과

목적: osteoclastogenesis에서 단백질 트라이어드 RANK-RANKL의 중요한 역할은 골다공증에 대한 약물의 합리적인 개발을 위해 그들의 결합을 중요한 목표로 만들었습니다.최근 leucine-rich repeat-containing G-protein-coupled receptor 4 (LGR4, GPR48로도 불림)가 RANKL에 대한 또 다른 수용체 인 것으로 보고되었다. LGR4는 RANKL에 결합하여 파골 세포 분화 동안 정식 RANK 신호 전달을 억제하기 위해 RANK와 경쟁한다.이를 바탕으로 RANKL과 RANKL 복합체의 결정 구조를 기반으로 RANKL을 변이시켜 RANK 신호가없는 LGR4 신호 전달이 파골 세포 생성 억제에 관여하는지 여부를 조사 하였다.

실험 및 방법: 개념 증명으로서, 돌연변이 RANKL은 RASKL- 유도 된 마우스 모델에서 GSK-3β인산화의 자극, NFATc1 전좌의 억제 및 TRAP 및 OSCAR의 mRNA 발현 및 TRAP 활성 및 골 흡수를 주도 하였다.

결과: 돌연변이 RANKL이 골다공증 치료제에 대한 부작용이 결여 된 RANKL에 의한 비교 억제에 의해 골다공증 치료제가 RANKL에 유도 된 파골 세포 형성을 억제 할 가능성이 있음을 입증 하였다.분석결과 골 형성이 가장 빠르게 촉진되었음을

관찰할 수 있었고, Type-1 Collagen 및 Osteocalcin 단백질 발현의 증가를 유도하였음을 알 수 있었다.

색인단어: mutative RANKL, RANK, 파골세포, 골다공증, 면역요법

Ⅰ. INTRODUCTION

Bone homeostasis is maintained by a balance between bone resorption by osteoclasts and bone formation by osteoblasts (1,2). Excessive osteoclast activity leads to an imbalance between bone resorption and formation, which is often observed in patients with osteoporosis(3,4). RANKL(Receptor activator of nuclear factor kappa-B ligand) is an essential cytokine in osteoclast differentiation. RANKL is the key molecule that regulates the differentiation and function of osteoclasts (5). The drugs most commonly used to treat osteoporosis, such as Alendronate (Binosto, Fosamax) Risedronate (Actonel, Atelvia) Ibandronate (Boniva) Zoledronic (Reclast, Zometa) is bisphosphonates. (6-8). These drugs are commonly used to decrease bone resorption by inhibiting the activity of osteoclasts (9,10). However, long-term administration is known to cause side effects such as jaw bone necrosis
and femoral fracture (11). To overcome these kind of side effect, OPG-Fc fusion protein capable of inhibiting RANKL activity and RANKL antibody were developed, and RANKL antibody with superior effect in pharmacokinetics was introduced denosumab and approved as a therapeutic agent for osteoporosis and is used clinically.

Targeting OPG-Fc decoy receptor RANKL inhibits osteoclastogenesis.This specific target treatment method is suggested as a good method.Among them, denosumab is introduced to chronic patients with osteoporosis when treated with denosumab, it has been reported to reduce bone resorption and prevent skeletal complications compared to continuing bisphosphonate treatment. Denosumab is a fully human monoclonal antibody to the receptor activator of nuclear factor-κB ligand (RANKL) which blocks its binding to RANK, inhibiting

the development and activity of osteoclasts, followed by suppression of bone resorption. But Side effects include hypocalcemia, infection, and skin reactions. In addition, because the drug inhibits bone turnover, it may also lead to jaw necrosis.

Recently, Leucine-rich repeat-containing G-protein-coupled receptor 4 (LGR4, also called GPR48) is introduced to another receptor of RANKL (12,13). LGR4 competes with RANK to bind RANKL and suppresses canonical RANK signaling during osteoclast differentiation (14). RANKL binding to LGR4 activates the Gαq and GSK3-β signaling pathway, an action that suppresses the expression and activity of nuclear factor of activated T cells, cytoplasmic, calcineurin dependent 1 (NFATC1) during osteoclastogenesis(15-17). In addition, RANKL-RANK-NFATc1 signaling during osteoclast differentiation can directly induce the expression of LGR4, which competes with RANK for RANKL binding in osteoclast lineage cells(18,19).

We hypothesize that the novel peptide modified from RANKL bind to LGR4 but not RANK could inhibit osteoclastogenesis by inhibiting RANKL-RANK signaling. Treatment of mRANKL-MT3 with mRANKL-MT3 in osteoclasts, measurement of differentiation and production of osteoclasts by TRAP analysis and TRAP staining, intracellular signal transduction through Western blot analysis, and differentiation factors by q-PCR analysis Expression check transcription factor, we examine the effect of mRANKL- MT3 on osteoclast differentiation and inhibition. In addition, RANKL-induced osteoporosis rats are examined for the inhibitory effect of mRANKL- MT3 on osteoclasts.

Therefore, this study aimed to confirm the possibility of novel peptide as an agent for osteoporosis treatment by clarifying the effect and mechanism of action on osteoclast differentiation and bone resorption(20)

II. MATERIALS AND METHODS

1. RANKL variant production by Site-directed mutagenesis

The polymerase chain reaction (PCR) product was cloned into the NdeI/XhoI site of pGEX-4T-1 vector (Promega, Madison, WI, USA) and mutations at positions 180, 189-190, and 223-224 were introduced using megaprimers (Extended data Table 1). The PCR product was transformed into *Escherichia coli* BL21-Gold competent cells (Agilent, Santa Clara, CA, USA) by electroporation (5 ms, 12.5 kV/cm) and the transformed *E. coli* cells were cultivated in Luria-Bertani (LB) broth with ampicillin (50 μg/mL, T&I, Daejeon, Korea). Plasmid was purified with the QIAprep Spin Miniprep Kit (Qiagen, Valencia, CA, USA). The cloned product was confirmed with commercial sequencing service (SolGent Co., Daejeon, Korea). All sequence analyses were carried out using programs in Vector NTI Advance 9.1.0 (Invitrogen, Carlsbad, CA, USA).

2. mRANKL-MT3 purification

The recombinant plasmid carrying mutant RANKL was expressed from a single *E. coli* BL21-Gold colony using previously described methods . Briefly, a single colony carrying the recombinant plasmid was inoculated in 20 mL LB medium supplemented with ampicillin (50 μg/mL) and incubated at 37 ° C with agitation at 200 rpm for 15 h. Ten milliliters of this culture was inoculated in an Erlenmeyer flask containing 1 L of LB medium with 50 μg/mL of ampicillin. The

cells were incubated at 37 ° C and 180 rpm until the absorbance at 600 nm (OD600) reached a value of ≈1.0 Isopropyl β-D-1-thiogalactopyranoside (IPTG) was added at concentrations of 0.1 mM to induce protein expression, and the cells were further cultured for 6 h. After induction, cultures were centrifuged at 5600×g for 20 min at 4 ° C and cell pellets were stored at -20 ° C. To prepare a bacterial lysate for affinity column chromatography, the pellet was resuspended in a lysis buffer (phosphate buffered saline [PBS], 1 mM ethylenediaminetetraacetic acid (EDTA) [pH 8.0], 0.1% Tween 20, 20 uM phenylmethylsulfonyl fluoride [PMSF]) and sonicated (Vibra Cell VCX500; Sonics & Materials, Inc., Newtown, CT, USA) on an ice bed. After sonication, recombinant GST fusion RANKL was purified using a Glutatione Sepharose™ 4M resin column (GE Healthcare, Uppsala. Sweden) in accordance with the manufacturer's protocol. The eluted protein was dialyzed against a dialysis buffer (20% v/v glycerol in phosphate buffered saline [PBS]) in a 10,000 MW Slide-A-Lyzer Dialysis cassette (Thermo Fisher Scientific, Waltham, MA, USA). The purified protein was vacuum concentrated (Savant Instruments, Holbrook, NY, USA) and analyzed with sodium dodecyl sulfate polyacrylamide gel electrophoresis (SDS-PAGE). Protein concentrations to calculate yields were determined with the Bradford assay. For endotoxin removal, the High-Capacity Endotoxin removal Resin (Pierce Biotechnology Inc., Rockford, IL, USA) was used to remove contaminating LPS from the recombinant protein. The endotoxin level in the RANKL preparation was 0.48 EU/ml resulting in 0.92 EU per 1 mg administered to each mouse. Recombinant protein samples were resolved by

electrophoresis. After separation, the gel was stained with Coomassie brilliant blue G-250. To determine the purity and recovery rate of the recombinant protein, a stained gel loaded with a fixed amount of protein was imaged using a digital scanner (EPSON, USA) at 300 dpi.

3. TRAP assay

Bone marrow cells were flushed from tibias and femurs of 6-8 week-old female C57BL/6 mice, cultured in alpha-MEM containing 10% FBS and 30 ng/ml M-CSF (R&D systems, Minneapolis, MN, USA) after treating with RBC lysis buffer (Gibco, Gaithersburg, MD, USA). After 3 day incubation, non-adherent cells were removed and adherent cells were used as bone marrow macrophages (BMMs). Subsequently, Osteoclast differentiation was induced by addition of 30 ng/ml M-CSF and various concentration of RANKL (R&D systems) and in the present or absent of antibody or antiserum for a further 4 days. The multinucleated cells were stained for tartrate-resistant acid phosphatase (TRAP) (KAMIYA BIOMEDICAL Co., Seattle, WA, USA) and more than 3 nuclei TRAP-positive cells were identified as osteoclasts.

4. Bone resorption assay

To observe the bone resorption in vitro, BMMs were cultured to_Corning®_ Osteo Assay Surface 96-well Multiple Well Plates (Sigma, Cat no. CLS3988) with M-CSF plus RANKL for 6 days with or without different concentration of antibody, then the plates were washed with pure water.

5. Quantitative Reverse transcription- PCR (qPCR) analysis

Total RNA was extracted from BMMs using TRIzol® reagent (Invitrogen; Thermo Fisher Scientific, Inc.). cDNA was synthesized from 2 μg total RNA using the ReverTra Ace® qPCR RT Master Mix (TOYOBO). mRNA levels were measured via qPCR, RT-PCR, and the GAPDH gene was used as an endogenous control.

6. Western blot analysis

Cells were serum starvated for 8 hours and treated with 2 μg / ml, mRANKL-MT3 at 5, 15 and 30 minute intervals. cells were lysed in 5× SDS-loading buffer with protease and phosphatase inhibitors cocktails. Approximately 30 mg of tissue lysate was separated via 10% sodium dodecyl sulfate-polyacrylamide gel electrophoresis (SDS-PAGE) and transferred onto a polyvinylidene difluoride (PVDF) membrane (Amersham, Piscataway, NJ, USA). Each membrane was blocked for 30 min with a blocking solution containing 5% skim milk in Tris-buffered saline containing Tween-20 (TBST, 2.42 g/l Tris-HCl, 8 g/l NaCl, 0.1% Tween-20, pH 7.6) and rinsed with TBST. The membrane was incubated overnight at 4°C with appropriate primary antibodies, including p-Akt (1:1,000; 9271S; Cell Signaling Technology) Akt (1:1,000; 9272S; Cell Signaling Technology), p-p38 (1:1,000; 9211S; Cell Signaling Technology), p38 (1:1,000; 9212S; Cell Signaling Technology), p-ERK (1:1,000; 9101S; Cell Signaling Technology), ERK (1:1,000;9102S; Cell Signaling Technology), p-JNK (1:1,000; 9251S; Cell Signaling Technology), JNK (1:1,000; 9252S; Cell Signaling Technology), p-GSK-

3β (1:1,000; 9336S; Cell Signaling Technology), GSK-3β (1:1,000; 9315S; Cell Signaling Technology), p-Src (1:1,000; 2105S; Cell Signaling Technology), Src (1:1,000; 2108S; Cell Signaling Technology), RANK (1:1,000; 4845S; Cell Signaling Technology), Gαq (1:1,000; 14373S; Cell Signaling Technology) and LGR4 (1:500; MBS468030; MyBioSource). A mouse monoclonal immunoglobulin G (IgG) specific for glyceraldehyde-3-phosphate dehydrogenase (GAPDH, 1:1,000; 2118S; Cell Signaling Technology) was used as a control. The membrane was rinsed with TBST, and protein immunoreactivity was detected using an enhanced chemiluminescence detection kit (ECL, Amersham).

7. Seperation of nuclear and cytosol

Add 500 μl of Buffer A to the BMMs and scratch by adding the protease inhibitor cocktail. After 10 min on ice, centrifuge for 10 min at 3,000 rpm at 4 ° C. Remove supernatant and store In the case of Buffer B, the pellet is resuspended in 374 μl and added to 26 μl of 4.6 M NaCl to homogenize with a total of 15 strokes in a glass homogenizer and then centrifuged at 24,000 x g for 20 minutes at 4 ° C. for 30 minutes on ice. Separate nuclear and cytosol was assayed by western blot.

8. Confocal microscopic analyses

BMMs were plated in 96-well plates and stimulated with 250 ng / ml M-CSF and 250 ng/ml RANKL for 3 days in the absence.

Cells were fixed with 4% PFA for 10 min, permeated with 0.1% Triton X-100

for 5 min and stained with DAPI.Immunolabeled cells were counterstained with 4',6'-diamidino-2-phenylindole (DAPI) provided in ProLong Gold antifade mounting medium (Invitrogen; Thermo Fisher Scientific, Inc., Waltham, MA, USA) to visualize nuclear morphology. Digital images were acquired at the Korea Basic Science Institute Gwangju Center using a TCS SP5 AOBS laser-scanning confocal microscope (Leica Microsystems, Heidelberg, Germany).

9. Micro-CT imaging and data acquisition

Micro-CT scanning for the distal femur was distally initiated at the level of growth plate using a Quantum GX micro-CT imaging system (PerkinElmer, Hopkinton, MA, USA) located at the Korea Basic Science Institute in Gwangju, Korea. Scanning X-ray source was set to levels of 90 kV and 88 mA with a field of view of 10 mm (voxel size, 20 μm; scanning time, 4 min). The 3D imaging was represented with a 3D Viewer, an existing software within the Quantum GX. The resolution was set at 4.5 μm and images were obtained. Following scanning, the structural parameters for trabecular bone were analyzed with Analyze 12.0 software (AnalyzeDirect, Overland Park, KS, USA). The mineral density of the femur was estimated using a hydroxyapatite (HA) phantom (QRM-MicroCT-HA, Quality Assurance in Radiology and Medicine GmbH, Germany), scanned using the same parameters. Bone mineral density (BMD), % of bone volume (bone volume/tissue volume, %), trabecular number (Tb. N.), trabecular separation (Tb. Sp.), and trabecular thickness of femurs were

calculated using the ROI tool. The value of parameters was shown as mean ± standard deviation (SD).

10. Histological analysis of mouse tissues

Mouse Femur tissues were fixed in cold 4% PFA. Bone tissue was first decalcified using a 0.5 M EDTA solution before processing onto histological slides. Decalcified bones were cut at the midpoint and embedded in paraffin blocks. Tissues were stained with hematoxylin and eosin (H&E) stain, and images were acquired using an ECLIPSE Ts2R inverted microscope (Nikon, Tokyo, Japan). TRAP staining

III. RESULTS

1. Effect of mutant RANKL on osteoclast differentiation in vitro

To evaluate the inhibitory effect of mRANKL-MT3 on osteoclastogenesis in vitro, mRANKL-MT3 was treated dose dependently in the presence with mRANKL-WT on BMMs. The BMMs differentiated into mature, TRAP positive, multinucleated osteoclasts, which were significantly decreased in dose dependently in mRANKL-MT3-treated group. (Fig. 1a, 1b). Also, the inhibition of osteoclast activity of mRANKL-WT and mRANKL-MT3 was confirmed through bone resorption assay on hydroxyapatite plate. It was observed that bone resorption pit was decreased by dose dependent manners and activity of osteoclast in the same concentration of mRANKL-MT3 treated BMMs was significantly inhibited (Fig 1c, 1d)

2. Effect of mutant RANKL on mRNA expressions in related with osteoclastogenesis

To evaluate the Effect of mutant RANKL on mRNA expressions in related with osteoclastogenesis,we investigated the expression of several osteoclast-specific genes both at the mRNA levels using RT-qPCR assays. (Fig. 1a) in a competition inhibition assay using mRANKL-MT3 Significant reductions in DC-STAMP and Cathpsin-k were observed early time points. Significant reductions in OSCAR and ATP6V0D2 were observed middle stage. a significant reduction in NFATc1 and TRAP and C-src was observed late stage. (Fig. 1b) Overall, these results demonstrate that RANKL-induced osteoclasts were affected by competitive inhibition by treatment with mRANKL-MT3.

3. Effect of mutant RANKL on RANK-RANKL/LGR4-LANKL signaling cascade

To evaluate the Effect of mutant RANKL on RANK-RANKL/LGR4-LANKL signaling cascade, We validated that RANK and LGR4 signaling cascade in a time-dependent by Treatment of mRANKL-WT induced MAPK, AKT, src, and GSK-3β phosphorylation.(Fig. 3a) However, mRANKL-MT3 treatment in the presence of mRANKL-WT significant inhibition of MAPK, AKT, src, and GSK-3β phosphorylation Considering this result, we demonstrated that mRANKL-MT3 could totally block RANKL-RANK signaling as well as LGR4 signaling.(Fig. 3b)

4. Effect of mutant RANKL on NFATc1 translocation to nucleus

To evaluate the Effect of mutant RANKL on NFATc1 translocation to nucleus,we examined the effect of mRANKL-MT3 on the nuclear localization of NFATc1. NFATc1 nuclear translocation was not detected in mRANKL-WT. However, in the presence of mRANKL-WT, mRANKL-MT3 resulted in significant inhibition of NFAc1 translocation. NFATc1 was present in the mRANKL-WT treated BMM nuclei, In the presence of mRANKL-WT, but was not detected in the nuclei and cytosol of the mRANKL-MT3 treated BMM nuclei.(Fig 3c)

These results further support that mRANKL-MT3 inhibits osteoclast formation stimulated by mRANKL-WT and can be considered an effective comparative inhibitor for RANKL.(Fig 3d)

5. Effect of mutant RANKL on RANKL-induced mice

To investigate the effect of mtRANKL on bone lysis, mRANKL-MT3 treatment in the presence of mRANKL-WT were administered to healthy mice and the femur bones were examined by microCT. Mice with mRANKL-WT only received significant bone loss in mice. but mice with in the presence of mRANKL-WT, mRANKL-MT3 treated showed little bone loss.(Fig 4a) BMD, BV / TV, Tb.Th, BV. Ct.Th and other bone scores were assessed by quantitative micro CT. As expected, BMD, BV / TV and Tb.Th decreased. in the presence of mRANKL-WT mice, it was significantly recovered by mRANKL-MT3 treatment, and these results clearly demonstrate the therapeutic effect of mRANKL-MT3 against osteoporosis. (Fig 4b)

6. Effect of mRANKL-WT+mRANKL-MT3 decreased the formation of osteoclastin mice

In a histological assay by H&E staining in mRANKL-WT group the trabecular bone was found to be thin and the network structure was severely disrupted and fragmented (Fig. 5a).

However, the belonging to mRANKLWT+mRANKL-MT3 group exhibited a normal arrangement pattern with a thick and dense network with minimal spaces, as in control group. In addition, we stained histological sections of TRAP staining experiments showed that while mRANKL-WT + mRANKL-MT3 group treated appear present fewer TRAP-positive osteoclasts compared to mRANKL-WT group.(Fig.5b) To quantify data, we calculated the ratio of TRAP-positive area to trabecular

bone surface (OCs/BS %) and the ratio of osteoclast number to bone area (OCs/mm2) for each group Quantification results confirmed that both OCs/BS % and OCs/mm2 values in mRANKL-WT+mRANKL-MT3 group treated were significantly smaller than those of mRANKL-WT group.(fig.5c,5d)

IV. Discussion

Osteoporosis is a disease that is characterized by low bone mass, deterioration of bone tissue, and disruption of bone microarchitecture: it can lead to compromised bone strength and an increase in the risk of fractures.

Treatment of osteoporosis may use drugs that increase bone formation or decrease bone resorption. Drugs that increase bone formation have also been developed and are being studied, The most used drugs are drugs that inhibit bone resorption (bisphosphate, SERM, calcitonin, estrogen), and calcium, vitamin D, etc. are also frequently used as supplements. Therefore, the present study is investigated whether the trial of treatment is within reach using by the of RANKL which is the key molecule of osteoclastogenesis.

Clinically, denosumab targets OPG-Fc decoy receptor RANKL as an OPG-Fc fusion protein and RANKL antibody capable of regulating the development and function of osteoclasts and inhibiting RANKL activity, as RANKL-RANK signaling is targeted. It can inhibit osteoclastogenesis. Denosumab is introduced to chronic patients with osteoporosis when treated with denosumab, it has been reported to reduce bone resorption and prevent skeletal complications compared to continuing bisphosphonate treatment.

Therefore, Considering RANKL-RANK signaling regulates the development and function of osteoclast and the application of denosumab (human anti-RANKL mAb) in clinical therapies of osteoporosis and bone loss caused by have been treatment, designing and validating a novel peptide targeting RANKL is theoretically possible. The LGR4 is announced a novel receptor of RANKL and it inhibits RANKL-induced osteoclast differentiation by blocking RANK-TRAF6

signaling, as well as through Gαq and GSK3-β mediated inhibition of NFATC1. Here, a new mRANKL-MT3 mutated so as not to bind to RANK is a competitive inhibitory agent that inhibits Osteoclastogenesis by binding to the LGR4 receptor. It is believed that it can inhibit osteoclast formation

In the present study, the treatment of mRANKL-MT3 inhibited osteoclast differentiation in the presence of wild type of RANKL in vitro, which suggests that this may be a direct active strategy for the treatment of osteoporosis and other bone-resorption diseases in clinics. Our data implicate LGR4 as a pivotal player of a negative-feedback mechanism to control osteoclast activities. The LGR4 signaling cascade activated Gαq and GSK-3β signaling pathways that act to inhibit the expression and activity of nuclear factors of NFATC1 during osteoclast differentiation. Furthermore, LGR4-extra cellular domain have known to have a lower binding affinity than OPG with RANKL, and that it is considered that LGR4-mRANKL-MT3 binding had little physiological effect on osteoclast differentiation in normal mice, which suggests that the minimal effect of LGR4-mRANKL-MT3 protein in normal mice could be due to endogenous OPG competition.

Especially in the previous study, Lgr4 expression is reported to be increased during osteoclast differentiation and peaked in mature osteoclasts; targeting LGR4 thus may affect mature osteoclasts but have less effect in BMMs and pre-osteoclasts, and so reduce side effects involved in the treatment of osteoclast-related diseases by mRANKL-MT3.

In summary, The first one novel peptide is mRANKL-MT3 induces the Competitive inhibiton effect against RANKL during osteoclastogenesis. And the second one is mRANKL-MT3 itself involves LGR4 mediation of RANKL-NFATC1 signaling cascade and negative-feedback mechanism to control osteoclast activities.

V. Conclusion

The critical role of the protein triad, RANK-RANKL, in osteoclastogenesis has made their binding an important target for the rational development of drugs against osteoporosis. Recently, it is reported that leucine-rich repeat-containing G-protein-coupled receptor 4 (LGR4, also called GPR48) is another receptor for RANKL. LGR4 competes with RANK to bind RANKL and suppresses canonical RANK signaling during osteoclast differentiation. Based on this, the RANKL was mutated the point in based on the crystal structure of the complex of RANKL and its counterpart receptor RANK and it is investigated whether the LGR4 signaling without RANK signal could be involved in inhibition of osteoclastogenesis. As a proof of concept, mutant RANKL led the stimulation of GSK-3beta phosphorylation, inhibition of NFATc1 translocation and mRNA expression of TRAP and OSCAR and TRAP activities and bone resorption, subsequently in RANKL-induced mouse models. The results demonstrated that the mutative RANKL has a possibility to therapeutic agent for osteoporosis to inhibit the RANKL-induced osteoclastogenesis by comparative inhibition with RANKL in which lacks toxic side effects for the treatment of osteoporosis.

REFERENCES

1. Tanaka Y, Nakayamada S, Okada Y. Osteoblasts and osteoclasts in bone remodeling and inflammation. Curr Drug Targets Inflamm Allergy 2005;4:325-8
2. Landesberg R, Woo V, Cremers S, Cozin M, Marolt D, Vunjak-Novakovic G, et al. Potential pathophysiological mechanisms in osteonecrosis of the jaw. Annals of the New York Academy of Sciences 2011;1218:62
3. Feng X, McDonald JM. Disorders of bone remodeling. Annu Rev Pathol 2011;6:121-45
4. Bi H, Chen X, Gao S, Yu X, Xiao J, Zhang B, et al. Key triggers of osteoclast-related diseases and available strategies for targeted therapies: A review. Frontiers in medicine 2017;4:234
5. Hofbauer L, Kuhne C, Viereck V. The OPG/RANKL/RANK system in metabolic bone diseases. Journal of Musculoskeletal and Neuronal Interactions 2004;4:268
6. Penning-van Beest F, Erkens J, Olson M, Herings R. Loss of treatment benefit due to low compliance with bisphosphonate therapy. Osteoporosis international 2008;19:511-7
7. Manfredi M, Merigo E, Guidotti R, Meleti M, Vescovi P. Bisphosphonate-related osteonecrosis of the jaws: a case series of 25 patients affected by osteoporosis. International journal of oral and maxillofacial surgery 2011;40:277-84
8. Bachrach LK, Ward LM. Clinical review: bisphosphonate use in childhood osteoporosis. The Journal of Clinical Endocrinology & Metabolism 2009;94:400-9

9. Mühlbauer RC, Bauss F, Schenk R, Janner M, Bosies E, Strein K, et al. BM 21.0955, a potent new bisphosphonate to inhibit bone resorption. Journal of bone and mineral research 1991;6:1003-11

10. Carano A, Teitelbaum S, Konsek J, Schlesinger P, Blair H. Bisphosphonates directly inhibit the bone resorption activity of isolated avian osteoclasts in vitro. The Journal of clinical investigation 1990;85:456-61

11. Kim T-W, Yoshida Y, Yokoya K, Sasaki T. An ultrastructural study of the effects of bisphosphonate administration on osteoclastic bone resorption during relapse of experimentally moved rat molars. American journal of orthodontics and dentofacial orthopedics 1999;115:645-53

12. Jönsson B, Ström O, Eisman JA, Papaioannou A, Siris E, Tosteson A, et al. Cost-effectiveness of denosumab for the treatment of postmenopausal osteoporosis. Osteoporosis international 2011;22:967-82

13. Kostenuik PJ, Nguyen HQ, McCabe J, Warmington KS, Kurahara C, Sun N, et al. Denosumab, a fully human monoclonal antibody to RANKL, inhibits bone resorption and increases BMD in knock-in mice that express chimeric (murine/human) RANKL. Journal of Bone and Mineral Research 2009;24:182-95

14. Luo J, Yang Z, Ma Y, Yue Z, Lin H, Qu G, et al. LGR4 is a receptor for RANKL and negatively regulates osteoclast differentiation and bone resorption. Nature medicine 2016;22:539

15. Van Dam PA, Verhoeven Y, Jacobs J, Wouters A, Tjalma W, Lardon F, et al. RANK-RANKL Signaling in Cancer of the Uterine Cervix: A Review. International journal of molecular sciences 2019;20:2183

16. Matsumoto Y, Larose J, Kent OA, Lim M, Changoor A, Zhang L, et al.

RANKL coordinates multiple osteoclastogenic pathways by regulating expression of ubiquitin ligase RNF146. The Journal of clinical investigation 2017;127:1303-15

17. Kang IS, Kim C. NADPH oxidase gp91 phox contributes to RANKL-induced osteoclast differentiation by upregulating NFATc1. Scientific reports 2016;6:38014

18. Yi H. Identification and Characterisation of Lgr4/β-catenin Signalling in Acute Myeloid Leukaemic Stem Cells: University of New South Wales; 2016.

19. Renema N, Navet B, Heymann M-F, Lezot F, Heymann D. RANK-RANKL signalling in cancer. Bioscience reports 2016;36:e00366

20. Arnez MFM, Ribeiro LSN, Barretto GD, Monteiro PM, Ervolino E, Stuani MBS. RANK/RANKL/OPG expression in rapid maxillary expansion. Brazilian dental journal 2017;28:296-300

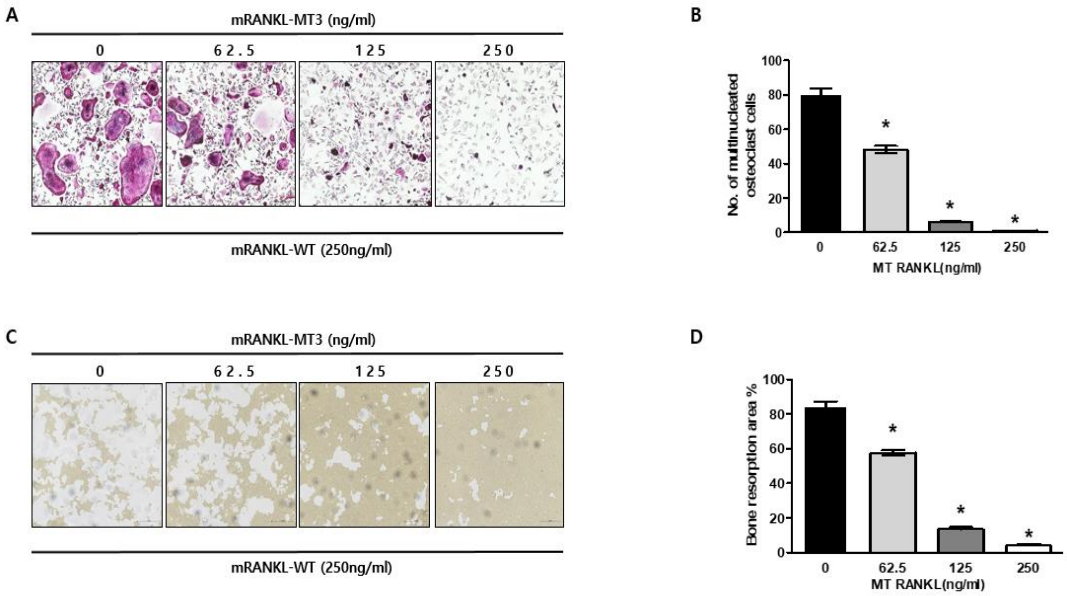

Figure 1. Effect of mutant RANKL(mRANKL-MT3) on osteoclast differentiation in vitro (a). Typical image of BMMs stained for TRAP (red) after treatment with various doses of mRANKL-MT3 (0, 62.5, 125, 250ng) (b). Numbers of multinucleated TRAP cells (BMMs) (red) (≥3 nuclei) in these cultures (n = 4); (c). BMMs were incubated on hydroxyapatite-coated plates with various doses of MT RANKL (0, 62.5, 125, 250ng). Remove cells attached to the plate and shoot with light microscope (d). Absorption area was quantified by Image J analysis. *** P, 0.001.

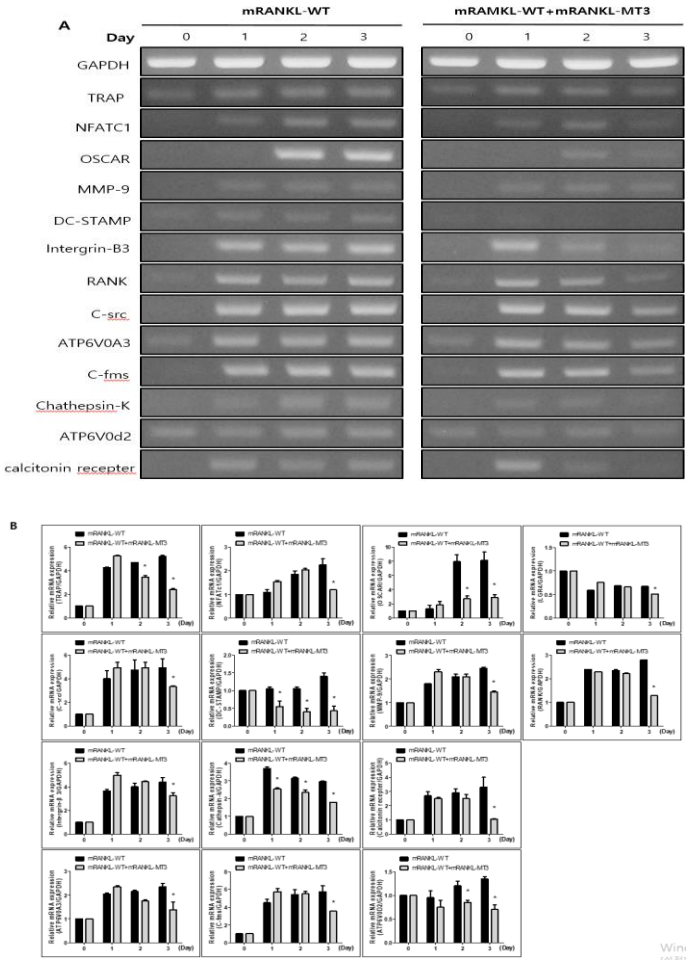

Figure 2. (a) mRANKL-MT3 inhibited RANKL-induced osteoclast gene expression, including NFATc1, TRAP and OSCAR. After pretreatment with various mRANKL-MT3 concentrations (0, 62.5, 125, 250ng), BMMs was incubated in induction medium for 3 days against the indicated medium.(b) were determined by RT-qPCR and normalized to the expression of GAPDH.These data are from three separate experiments and are expressed as the mean ± SD (#p< 0.05 compared with untreated control group; * p < 0.05, ** p < 0.01 compared with stimulated group treated with RANKL).

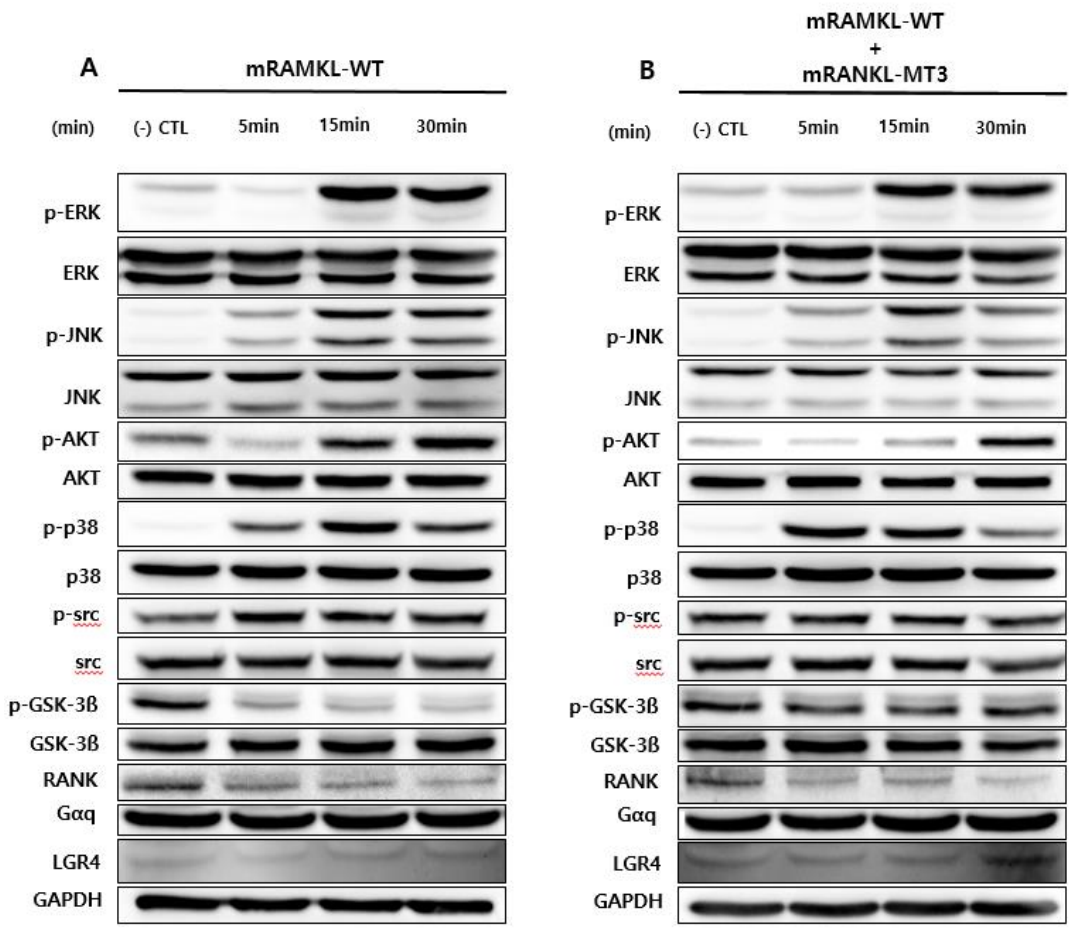

Figure 3. Inhibits p-GSK-3ß activation in RANKL- induced BMMs

(a). Cytokine- and serum-starved BMMs were exposed to mRANKL-WT (2μg/ml) over time. Total and phosphorylated signaling molecules were detected by Western blots. GAPDH served as loading control.

(b). Cytokine- and serum-starved BMMs were exposed to mRANKL-WT (2μg/ml)+MT RANKL (2μg/ml) over time. Total and phosphorylated signaling molecules were detected by Western blots. GAPDH served as loading control.

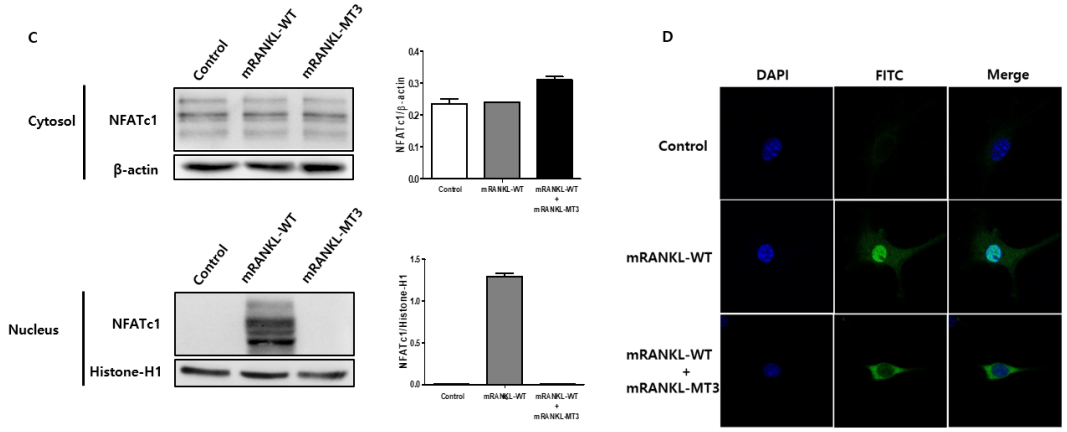

Figure 4. (c). BMMs were cultured for 24hr in the presence of M-CSF and RANKL. Nuclear and cytoplasmic fractions were prepared and analyzed using western blot analysis. (d). Suppression by mRANKL-MT3 of the M-CSF/RANKL stimulated expressions of the osteoclast-related transcription factor NFATc1, which are known to act as positive modulators of osteoclast differentiation.

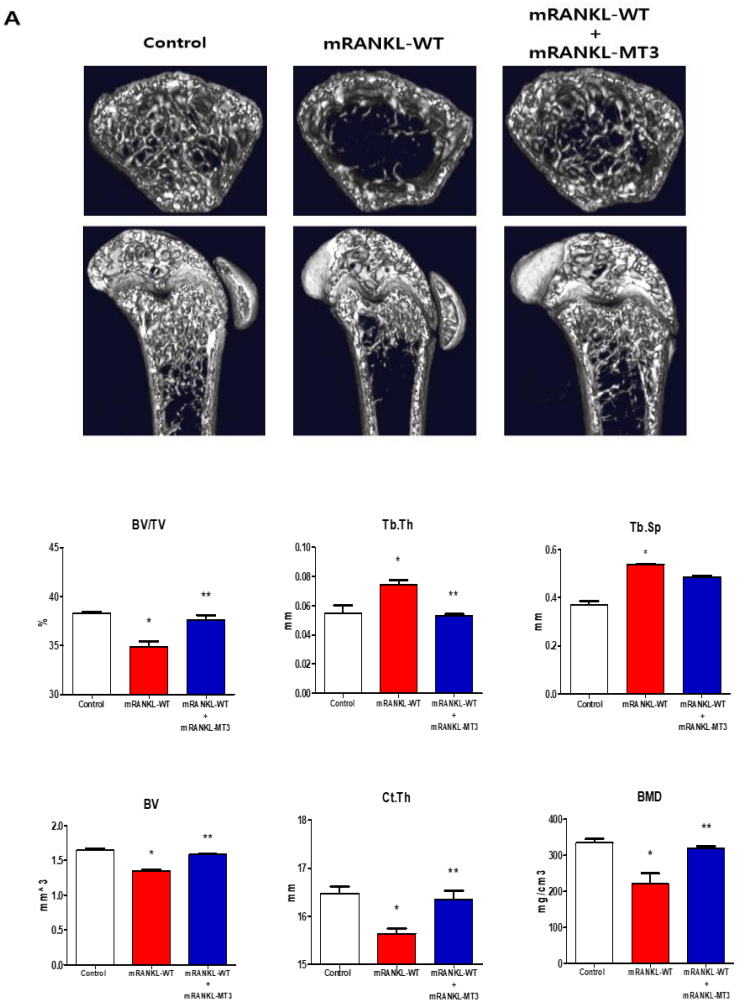

Figure 5. 3D microCT images of mouse femurs (a). Representative X-ray and microcomputed tomography images of the distal femurs of intact mice (control), RANKL-induced osteoporosis mice (vehicle),and mRANKL-MT3 treated RANKL-induced osteoporosis mice (b).) Bone volume/total volume (BV/TV), trabecular thickness (Tb.Th), trabecular spacing (Tb/sp), Bone Volume (BV), Cortical thickness (Ct/Th), Bone Mineral Density (BMD)

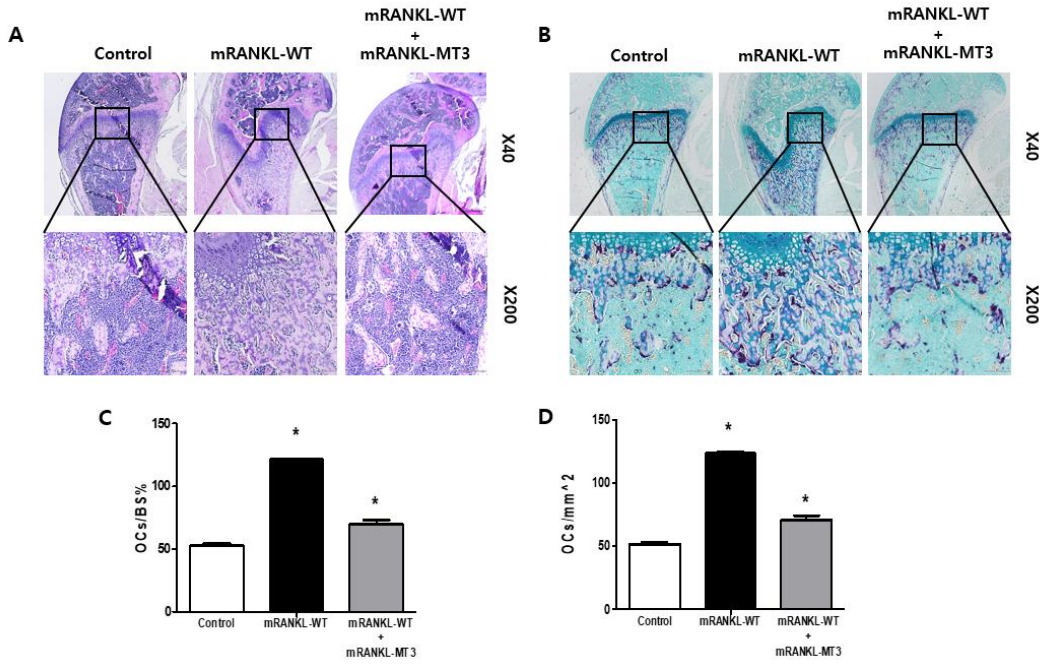

Figure 6. mRANKL-MT3 decreased the formation of osteoclastin mice (a) (b). Images of H&E and TRAP-stained (c). Quantification of osteoclast-covered surface over bone surface. (d). Osteoclasts number per mm2. Values were expressed as means ± SD. *P < 0.05. All the assays were repeated with at least 3 mice.